

Analysis of Signals Under Compositional Noise With Applications to SONAR Data

J. Derek Tucker^{*†}, Wei Wu^{*}, and Anuj Srivastava^{*}

^{*}Department of Statistics
Florida State University, Tallahassee, Florida 32306
Email: {dtucker,wwu,anuj}@stat.fsu.edu

[†]Naval Surface Warfare Center - Panama City Division
Panama City, FL 32407-7001
Email: james.d.tucker@navy.mil

Abstract—We consider the problem of estimation and classification of signals in presence of compositional noise, where the traditional techniques do not provide either a consistent estimator for signals or a robust distance for classification. We use a recently introduced comprehensive framework that: (1) uses a distance-based objective function for data alignment leading to a consistent estimator of signals, (2) combines the classical data and smoothness terms for signal registration in a natural fashion, obviating the need for an arbitrary relative weight, and (3) leads to warping-invariant distances between signals for robust clustering and classification. We use this framework to introduce two pairwise distances that can be used for signal classification: (1) a y -distance which is the distance between the aligned signals and (2) an x -distance, that measures the amount of warping needed to align the signals. This problem is motivated by automatic target recognition in underwater acoustic data, where the task of clustering and classifying objects using acoustic spectrum is complicated by the uncertainties in aspect angles at data collections. Small changes in the aspect angles corrupt signals in a way that amounts to compositional noise. We demonstrate the use of this framework in classification of spectral signatures in acoustic data and highlight improvements in signal classification over current methods.

Index Terms—compositional noise, functional data analysis, random warping, Riemannian methods, spectral signal classification, signal registration, SONAR

I. INTRODUCTION

The problem of underwater object detection and classification using sonar has attracted a substantial amount of attention [1]–[5]. This problem is complicated due to various factors such as variations in operating and environmental conditions, presence of spatially varying clutter, variations in target shapes, compositions and orientation. Moreover, bottom features such as coral reefs, sand formations, and vegetation may totally obscure a target or confuse the classification process. Consequently, a robust classification system should be able to quantify changes between the returns from the bottom and any target activity in sonar data. Thus, a robust system designed to mitigate false alarms in various clutter density scenarios will be desirable.

Considerable research has been devoted to the development of different detector and classification methodologies to de-

tect and classify underwater objects utilizing sonar imagery. Dobeck [1], [6] utilized a nonlinear matched filter to identify mine-size regions that match the target template in a side-scan sonar image. For each detected region, several features were extracted based on the size, shape, and strength of the target template. A stepwise feature selection process was then used to determine the subset of features that maximizes the probability of detection and classification. A k -nearest neighbor and an optimal discrimination filter classifier were used to classify each feature vector and the decisions of the two classifiers were fused to generate the final decision. In [2], the adaptive clutter filter detector in [7] was individually applied to three different sonar images varying in frequency and bandwidth. Final classification is done using an optimal set of features using a nonlinear log-likelihood ratio test where the decisions of the individual detector and classifier are fused. Recently in [4] we developed a new coherence-based detection framework for dual-sensor problem using Canonical Coordinate Analysis (CCA) that can be applied to the data collected using two disparate sonar systems. Using this method allows for the simultaneous detection and feature extraction of coherent target information among two sonar images.

These methods all use traditional synthetic aperture sonar (SAS) images which often provides high quality images of proud targets which are useful for image based detection, localization, and identification algorithms; however, this is not the case for buried targets where images are usually blurred with less structure definition, and hence, target identification from these images is more difficult. Generating acoustic color data products is one way to overcome these shortcomings. Acoustic color [8], [9] is a simple, spectral-based method that generates a normalized plot showing the strengths of the return signatures off an object in individual frequency bands at various aspects that may provide features useful for identification. The problem is then how does one do statistical analysis on these acoustic color images, which are essentially a two-dimensional function of frequency and aspect which represents target strength.

The solution to this problem is statistical functional data

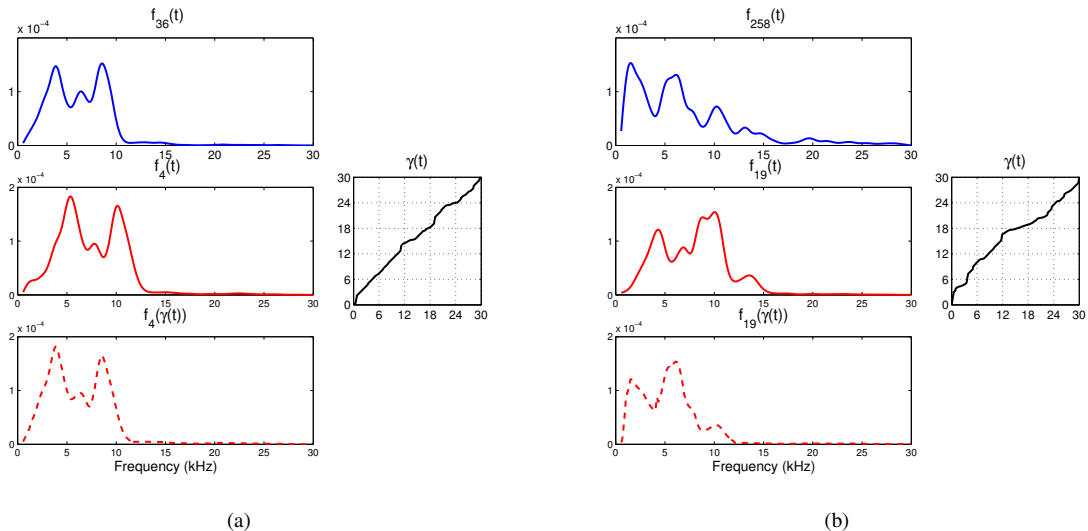


Fig. 1. (a) An example of frequency warping between two functions in the same class: f_{36} (upper panel), f_4 (middle panel, left) and $f_4 \circ \gamma$ (lower panel), where γ is the optimal warping (middle panel, right) between f_4 and f_{36} . (b) Same as (a) except that the functions f_{19} and f_{258} are in different classes.

analysis. However, one must be aware of a problem that manifests itself when doing classification and pattern recognition problems on this type of data. The data can be sensitive to sensor placement and alignment between samples over a target. Shown in Fig. 1(a) are two observed signatures (upper and middle panels) of the same target from two similar angles, one in blue line and one in red line, and it is easy to see shifts in peaks and valleys between the two signals. The bottom panel shows an alignment of red line to the blue line, denoting removal of warping noise, and the optimal warping function used here is shown in the right panel. Fig. 1(b) is same as (a) except that the two signatures are taken from two different target classes, where a more drastic warping is needed to align the signal. This motivates the use of a measure of warping as a separate metric by itself for target classification. In some instances, it may be relatively easy to decide how to warp functions from different samples for proper alignment, however this can become quite cumbersome for large data-sets and tends to be done in a supervised fashion. What we mean by warping is that a real-valued signal g on the frequency domain $[0, \Omega]$ is composed with a random warping function $\gamma_i : [0, \Omega] \rightarrow [0, \Omega]$ resulting in a nonlinear frequency-shift of the *locations* of peaks and valleys but not the heights of those peaks and valleys. In this paper, we present a method to overcome this problem by particularizing our previously developed framework developed in [10] to the estimation of spectral signatures for targets in presence of compositional noise, and evaluate it empirically in presence of both compositional and additive noise. Moreover, we introduce two metrics for classification of target classes from SONAR data: one of them is invariant to compositional noise and the other measures the warping itself.

This paper is organized as follows: Section II presents the current theory in elastic function alignment and presents

the Fisher Rao Metric and the corresponding classification metrics. Section III presents the results of this method when applied to acoustic color data presenting both the warping and separability of the metric in feature space. Finally, conclusions and observations are offered in Section IV.

II. FUNCTION REPRESENTATION AND ALIGNMENT

In this section, we adapt the theoretical framework presented in our recent report [11] and a conference paper [10] for automatic target recognition algorithms using SONAR data. This resulting framework achieves three important goals: (1) completely automated alignment of signals using nonlinear warpings, (2) estimation of underlying signals observed under random warpings, and (3) derivation of individual phase and amplitude metrics for comparing and classifying signals. For a more comprehensive introduction on this theory, including asymptotic theorems and estimator convergences, we refer the reader to [11].

First we introduce some notation. Let $f_1, f_2, \dots, f_n : [0, \Omega] \rightarrow \mathbb{R}$ be real-valued signals that are observed and let Γ be the set of boundary-preserving diffeomorphisms of the unit interval $[0, \Omega]$: $\Gamma = \{\gamma : [0, \Omega] \rightarrow [0, \Omega] \mid \gamma(0) = 0, \gamma(\Omega) = \Omega, \gamma \text{ is a diffeomorphism}\}$. Elements of Γ play the role of warping functions. That is, for any $\gamma \in \Gamma$, $f_i \circ \gamma$ denotes a composition or a warping of f_i by γ .

Let f be an acoustic signal viewed as a real-valued function with the domain $[0, \Omega]$. For concreteness, only functions that are absolutely continuous on $[0, \Omega]$ will be considered; let \mathcal{F} denote the set of all such functions. In practice, since the observed data is discrete, this assumption is not a restriction. Our first goal is to find a distance function that will be invariant to random warpings of the input functions. This distance is based on the Fisher-Rao Riemannian metric that was introduced in 1945 by C. R. Rao [12] to compare different probability distributions. An important attribute of this metric

is that it is preserved under identical warping of functions and Cencov [13] showed that it is the only Riemannian metric with this attribute. In order to keep the discussion simple, we will directly state the geodesic distance, denoted by d_{FR} , rather than deriving it from the Riemannian metric. It turns out that it is difficult to compute the distance d_{FR} from the first principles, but Srivastava et al [11] introduced a square-root representation that greatly simplifies this calculation. This function, $q : [0, 1] \rightarrow \mathbb{R}$, is called the *square-root velocity function* or SRVF of f , and is defined in the following form:

$$q(\omega) = \dot{f}(\omega) / \sqrt{|\dot{f}(\omega)|} .$$

It can be shown that if the function f is absolutely continuous, then the resulting SRVF is square-integrable. Thus, we will define $\mathbb{L}^2([0, \Omega], \mathbb{R})$, or simply \mathbb{L}^2 , to be the set of all SRVFs. For every $q \in \mathbb{L}^2$, the function f can be obtained precisely using the equation:

$$f(\omega) = f(0) + \int_0^\omega q(s)|q(s)|ds . \quad (1)$$

Thus, the representation $f \Leftrightarrow$ pair $(f(0)$ and $q)$ is invertible. If we warp a function f by γ , the SRVF of $f \circ \gamma$ is given by: $\tilde{q}(\omega) = (q, \gamma)(\omega) = q(\gamma(\omega))\sqrt{\dot{\gamma}(\omega)}$. The main motivation for using the SRVF for functional analysis is that under this representation, the complicated Fisher-Rao metric becomes the standard \mathbb{L}^2 metric and, therefore, the original form of this metric is not needed at all [11]. For any two functions f_1 and f_2 , define $d_{FR}(f_1, f_2) \equiv \|q_1 - q_2\|$, where q_1 and q_2 are the SRVFs of f_1 and f_2 , respectively. An important property of this distance is the following is that the Fisher-Rao distance d_{FR} is invariant to identical warping of the two input functions, i.e.,

$$d_{FR}(f_1, f_2) = d_{FR}(f_1 \circ \gamma, f_2 \circ \gamma) , \quad \forall \gamma \in \Gamma .$$

Why is this property important? The reason is that it leads to a distance between signals that is robust to their random warpings. This distance is defined as follows.

Definition 1 (Amplitude or y distance): For any two signals $f_1, f_2 \in \mathcal{F}$ and the corresponding SRVFs, $q_1, q_2 \in \mathbb{L}^2$, we define the amplitude or the y distance D_y to be:

$$D_y(f_1, f_2) = \inf_{\gamma \in \Gamma} \|q_1 - (q_2 \circ \gamma)\sqrt{\dot{\gamma}}\| .$$

An addition property of D_y is that it is invariant to the random warpings of the input signals, i.e., $D_y(f_1 \circ \gamma_1, f_2 \circ \gamma_2) = D_y(f_1, f_2)$ for all $\gamma_1, \gamma_2 \in \Gamma$.

It is quite possible that the level of warping may be different in different signal classes, and one can also use that for classification. Towards that goal, we define another metric D_x that compares relative warping needed to align any two signals. For any two functions $f_1, f_2 \in \mathcal{F}$ and the corresponding SRVFs, $q_1, q_2 \in \mathbb{L}^2$, let γ^* be given by:

$$\gamma^* = \operatorname{argmin}_{\gamma \in \Gamma} \|q_1 - (q_2, \gamma)\| = \operatorname{argmin}_{\gamma \in \Gamma} \|q_1 - (q_2 \circ \gamma)\sqrt{\dot{\gamma}}\| . \quad (2)$$

If $\gamma^* = \gamma_{id}$, then no warping is needed or the functions are perfectly aligned. Therefore, it makes sense to use the difference between γ^* and γ_{id} , in the set Γ , to define D_x .

We will define that value as the horizontal distance between functions:

Definition 2 (Phase or x distance): For any two functions $f_1, f_2 \in \mathcal{F}$, let γ^* be the optimal frequency warping function as given in Eqn. 2. Then, the horizontal distance between them, $D_x(f_1, f_2)$, is defined to be:

$$\begin{aligned} D_x(f_1, f_2) &= \sqrt{\Omega} \cos^{-1} \left(\left\langle \sqrt{\dot{\gamma}^*}, \sqrt{\dot{\gamma}_{id}} \right\rangle \right) \\ &= \sqrt{\Omega} \cos^{-1} \left(\int_0^\Omega \sqrt{\dot{\gamma}^*(\omega)} d\omega \right) . \end{aligned}$$

where $\langle \cdot, \cdot \rangle$ denotes the standard inner product operation in the \mathbb{L}^2 space.

III. EXPERIMENTAL RESULTS

In this section we describe some experimental results to demonstrate the classification of SONAR data using the distances D_y and D_x developed in the previous section. We choose the acoustic color data (spectral response) over spatial impulse response data to exploit resonances that occur in the frequency domain for different materials.

A. Data Description

The data set used in these experiments was collected at the Naval Surface Warfare Center Panama City Division (NSWC PCD) test pond. For a description of the pond and a similar experimental setup the reader is referred to [14]. The raw SONAR data was collected using a 1 - 30kHz LFM chirp and data was collected for nine proud targets that included a solid aluminum cylinder, an aluminum pipe, an inert 81mm mortar (filled with cement), a solid steel artillery shell, two machined aluminum UXOs, a machined steel UXO, a de-militarized 152mm TP-T round, a de-militarized 155mm empty projectile (without fuse or lifting eye), and a small aluminum cylinder with a notch. The aluminum cylinder is 2ft long with a 1ft diameter; while the pipe is 2ft long with an inner diameter of 1ft and 3/8 inch wall thickness. During the experiment the targets were placed with added uncertainty of their orientation.

The acoustic signals were generated from the raw SONAR data to construct target strength as a function of frequency and aspect angle. Due to the relatively small separation distances between the targets in the experimental setup, the scattered fields from the targets overlap. To generate the acoustic templates, SAS images were formed and then an inverse imaging technique was used to isolate the response of an individual target and to suppress reverberation noise. A brief summary of this process is as follows: The raw SONAR data is matched filtered and the SAS image is formed using the $\omega - k$ beamformer [15]. The target is then located in the SAS image and is then windowed around selected location. This windowed image contains the information to reconstruct the frequency signals associated with a given target

Amount of Smoothing	0	25	75	125	175
D_x	0.57	0.58	0.59	0.58	0.55
D_y	0.63	0.73	0.67	0.64	0.60
\mathbb{L}^2	0.43	0.44	0.45	0.45	0.44

TABLE I
CLASSIFICATION RATES VERSUS AMOUNT OF SMOOTHING APPLIED.

via inverting the $\omega-k$ beamformer [16] and the responses were aligned in range using the known acquisition geometry. For the nine targets, 2000 different data collections runs were done, and 1102 acoustic color templates were generated using the method described above from the data set. From the acoustic color maps, one-dimensional functional data was generated by taking slices at aspect value of 0° and therefore generating 1102 data samples.

B. Classification using Pairwise Distances

In this section we present experimental results for classification of signals using different metrics developed in this paper. We applied our metrics for classifying SONAR data containing $n = 1102$ SONAR signals with nine target classes and the numbers of observations in the nine classes are

$$\{n_i\}_{i=1}^9 = \{131, 144, 118, 118, 121, 119, 120, 114, 117\},$$

respectively. A selected subset of functions in each class is shown in Fig. 2. We observe that the original data is quite noisy, due to both the compositional and the additive noise, increasing variability within class and reducing separation across classes. This naturally complicates the task of target classification using SONAR signals.

To have a robust estimate of the SRVF $\{q_i\}$, we at first smooth the original signals $\{f_i\}$ using a standard box filter $[1/4, 1/2, 1/4]$. That is, numerically we update the signals at each discrete point by

$$f_i(\omega_k) \rightarrow \left(\frac{1}{4}f_i(\omega_{k-1}) + \frac{1}{2}f_i(\omega_k) + \frac{1}{4}f_i(\omega_{k+1}) \right).$$

To determine the effect of smoothing on the classification performance we conducted a small study on the number of times the smoothing filter is applied. Table I presents the classification performance versus applying the smoothing filter 0, 25, 75, 125, and 175 times. It is interesting to note that the performance is quite stable with respect to smoothing and smoothing 25 times gives slightly better performance. Hence, we use that level of smoothing for each signal for the rest of the analysis .

We first compute the standard \mathbb{L}^2 distance between each pair, i.e., $(\mathbb{L}^2)_{ij} = \|f_i - f_j\|$, $i, j = 1, \dots, n$. The matrix of pairwise \mathbb{L}^2 distances are shown as a gray scale image in Fig. 3(a). This image of the pairwise distances looks very noisy, underlying the difficulty of classification using SONAR data. Based on this distance matrix, we perform classification by using the LOO cross-validation on the standard nearest-neighbor method. It is found that the accuracy is 44.37%

(489/1102). Then we computed distances D_y and D_x between all pairs of signals and these distance matrices are shown as gray scale images in Fig. 3(b) and (c), respectively. Note that in theory D_x and D_y should lead to symmetric matrices but in practice, due to the numerical errors, these matrices are not exactly symmetric. So, we force them to be symmetric using $D_x \rightarrow (D_x + D_x^T)/2$, $D_y \rightarrow (D_y + D_y^T)/2$, where the superscript T indicates the transpose of a matrix.

In the image of D_y (Fig. 3(b)), we find that the pairwise distances are more structured than the \mathbb{L}^2 distances. We also perform classification using the LOO cross-validated nearest-neighbor based on the D_y distances. The accuracy turns out to be 72.87% (803/1102), a significant improvement over the result (44.37%) in the standard \mathbb{L}^2 distances. Interestingly, we find that the D_x distances also have strong indication of the target class in the data. In Fig. 3(c), we see that the D_x image has some clusters (dark squares) along the main diagonal. The classification accuracy by D_x turns out to be 58.35% (643/1102), which is also higher than the classification performance of the standard \mathbb{L}^2 norm in the function space.

Since D_x and D_y each only partially describe variability in the data, corresponding to phase and amplitude differences between the functions, there is a possibility of improvement if D_x and D_y are used jointly. One simple idea is to linearly combine these two distances and use the weighted distance to perform classification on the data. Here the amplitude and phase are being treated as two different “features” of the signals. To accurately represent the contribution from each distance, we at first normalize D_x and D_y by the maximum values in the matrices, respectively. That is, $D_x \rightarrow \frac{D_x}{\max D_x}$, $D_y \rightarrow \frac{D_y}{\max D_y}$. Then, for $\tau \in [0, 1]$, we define

$$D_\tau = \tau D_x + (1 - \tau) D_y.$$

D_τ is a weighted average of D_x and D_y with $D_0 = D_y$ and $D_1 = D_x$.

The next step is the estimation of an optimal τ . Towards this end, we randomly select 50% of the given signals as training data and evaluate the LOO classification performance for different values of τ . Since this selection is random, the resulting evolution is potentially random. Fig. 4(a) shows the performance profile versus τ for 100 randomly selected training data. An average of these curves is superimposed on the same plot (thick line). A histogram of the optimal values of τ for different random selections of the training data is shown in (b). Both these figures show that a broad range of τ values, from 0.3 to 0.7, all result in a decent increase in the classification performance over the individual metrics D_x and D_y , and the general pattern of increase is similar. In fact, if we use the full data and plot the LOO classification performance versus τ , we obtain the plot shown in (c). The overall shape (and the location of the maximizer) of this curve is very similar to the curves in (a) and underscores the independence of different observations. From this study, we select a value, say $\tau = 0.41$ and use that to perform LOO classification on the full data.

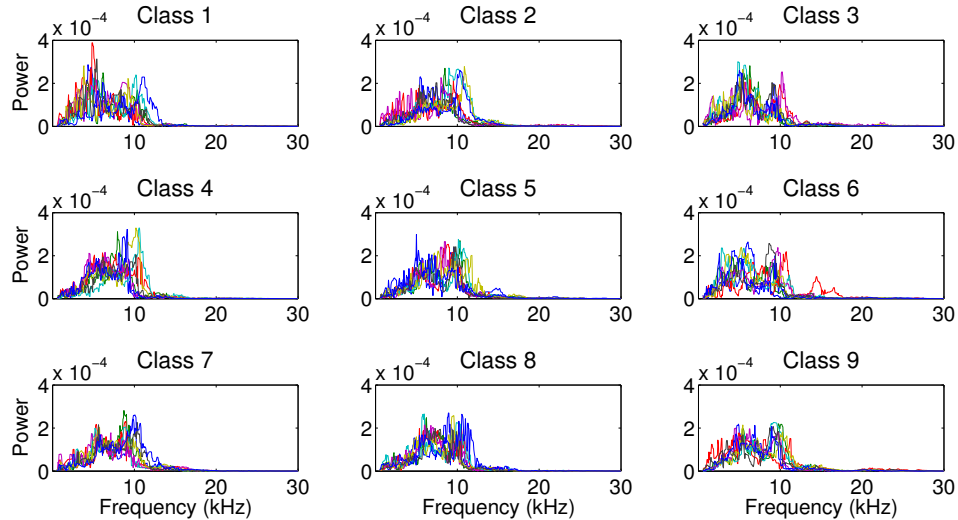


Fig. 2. Original SONAR functions in each of the 9 classes.

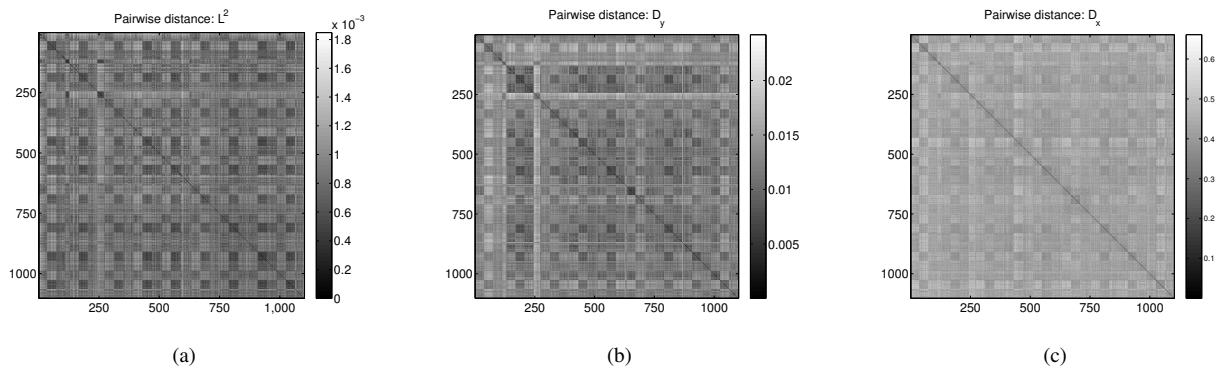


Fig. 3. The pairwise distances using the \mathbb{L}^2 (a), D_y (b), and D_x (c) metrics.

When $\tau = 0.41$, we get an accuracy at 76.13% (839/1102), which is higher than the accuracy in any of the \mathbb{L}^2 , D_y , and D_x distances. This indicates that the variability in the SONAR signals are better characterized when we separate the phase and amplitude variabilities, and better classification can be achieved when both variabilities are utilized.

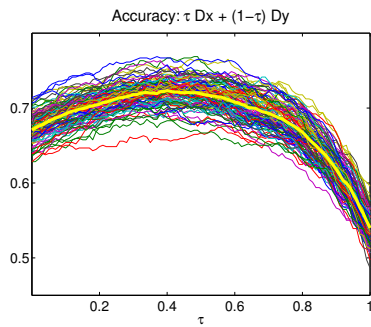
In order to compare with another existing idea, we compute the “naive” distance between any two signals presented in the previous section which is according to $(D_{Naive})_{ij} = \operatorname{argmin}_{\gamma \in \Gamma} \|f_i - f_j \circ \gamma\|$. We also perform the cross-validated nearest-neighbor using the D_{Naive} , and find that the accuracy is 63.70% (702/1102). This is slightly better than the accuracy by D_x , but worse than that by D_y . This indicates that even a simple-minded warping can help remove certain warping noise in the SONAR data, but the performance is not as good as a more formal SRVF-based warping.

Next we generated a cumulative match characteristic (CMC) curve for the distances D_x , D_y , D_τ ($\tau = 0.41$), D_{Naive} , and \mathbb{L}^2 . A CMC curve plots the probability of classification

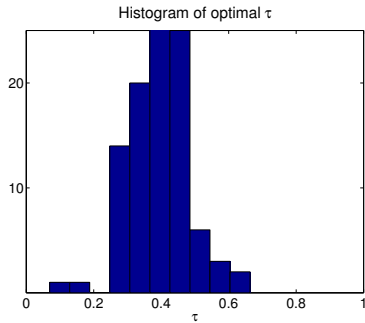
against the returned candidate list size and is presented in Fig. 5. Initially, D_y and D_τ outperform the other distances with D_{Naive} slightly outperforming D_x . After a slight increase in the returned list size D_x begins to outperform D_{Naive} and our method rapidly approaches over 90% classification rate, in contrast to the D_{Naive} and the standard \mathbb{L}^2 distances.

IV. CONCLUSIONS AND OBSERVATIONS

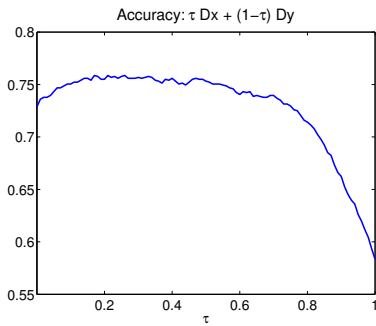
The statistical analysis and classification of targets using acoustic signatures is a challenging task. In particular, this task is complicated by the presence of compositional noise in the observed signals. We have proposed a comprehensive approach that solve the problem of estimating and comparing signals in unified framework, using a cost function that is eventually a warping-invariant distance between the two signals. This framework is applied to both the real and simulated data. It provides two distances – D_x and D_y – that can be used for classifying noisy signals using any metric-based classifier. We have used the leave-one-out classifier in this paper to demonstrate the improvements over traditional methods for



(a)



(b)



(c)

Fig. 4. (a) Evolution of classification performance versus τ for randomly selected training data. The average of these curves is drawn on the top. (b) The histogram of optimal τ values for different random selections of training data. (c) Overall performance versus τ for the full data.

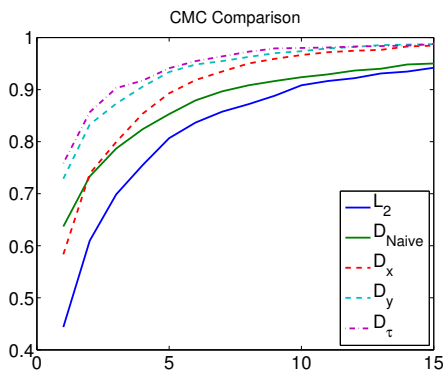


Fig. 5. CMC Comparison of L^2 , D_{Naive} , D_x , D_y and the weighted D_τ ($\tau = 0.41$) distances.

signal comparisons. In experiments involving real data we demonstrate a LOO performance of almost 76% which easily outperforms the standard L^2 distance (44%) and current methods using naive alignment (64%).

ACKNOWLEDGMENT

This work was supported by the Naval Surface Warfare Center Panama City Division In-house Laboratory Independent Research program funded by the Office of Naval Research (ONR) and ONR grant # N00014-09-1-0064. Approved for public release; distribution is unlimited.

REFERENCES

- [1] G. J. Dobeck, "Image normalization using the serpentine forward-backward filter: application to high-resolution sonar imagery and its impact on mine detection and classification," *Proc. SPIE*, vol. 5734, pp. 90–110, April 2005.
- [2] T. Aridgides and M. Fernandez, "Image-based ATR utilizing adaptive clutter filter detection, LLRT classification, and volterra fusion with application to side-looking sonar," *Proc. SPIE*, vol. 7664, pp. 1R–11R, March 2010.
- [3] N. Klausner, M. R. Azimi-Sadjadi, and J. D. Tucker, "Multi-sonar target detection using multi-channel coherence analysis," *Proc. of MTS/IEEE Oceans 2010 Conference*, pp. 1–7, Sept. 2010.
- [4] J. D. Tucker and M. R. Azimi-Sadjadi, "Coherence-based underwater target detection from multiple sonar platforms," *IEEE Journal of Oceanic Engineering*, vol. 36, no. 1, pp. 37–51, Jan 2011.
- [5] J. D. Tucker, J. T. Cobb, and M. R. Azimi-Sadjadi, "Generalized likelihood ratio test for finite mixture model of K-distributed random variables," *Proc of IEEE DSP/SPE 2011 Workshop*, pp. 443–448, Jan 2011.
- [6] G. J. Dobeck, "Fusing sonar images for mine detection and classification," *Proc. SPIE*, vol. 3710, pp. 602–614, April 1999.
- [7] T. Aridgides, P. Libera, M. Fernandez, and G. J. Dobeck, "Adaptive filter/feature orthogonalization processing string for optimal LLRT mine classification in side-scan sonar imagery," *Proc. SPIE*, vol. 2765, pp. 110–121, April 1996.
- [8] N. Intrator, N. Neretti, and Q. Huynh, "Sonar object discrimination via spectral density analysis," *Proc. of MTS/IEEE OCEANS 2004 Conference*, vol. 2, pp. 740–742, Nov 2004.
- [9] D. Miklovic and M. Bird, "Quantitative acoustic color displays for classification with broadband sonars," *Proc. of MTS/IEEE Oceans 1998 Conference*, vol. 1, pp. 592–597, Sept. 1998.
- [10] S. Kurtsek, A. Srivastava, and W. Wu, "Signal estimation under random time-warpings and nonlinear signal alignment," in *Proceedings of Neural Information Processing Systems (NIPS)*, 2011.
- [11] A. Srivastava, W. Wu, S. Kurtsek, E. Klassen, and J. S. Marron, "Registration of functional data using fisher-rao metric," *arXiv*, vol. 1103.3817v2, 2011.
- [12] C. R. Rao, "Information and accuracy attainable in the estimation of statistical parameters," *Bulletin of Calcutta Mathematical Society*, vol. 37, pp. 81–91, 1945.
- [13] N. N. Čencov, *Statistical Decision Rules and Optimal Inferences*, ser. Translations of Mathematical Monographs. Providence, USA: AMS, 1982, vol. 53.
- [14] S. Kargl, K. Williams, T. Marston, J. Kennedy, and J. Lopes, "Acoustic response of unexploded ordnance (UXO) and cylindrical targets and cylindrical targets," *Proc. of MTS/IEEE Oceans 2010 Conference*, pp. 1–5, 2010.
- [15] M. Soumekh, *Synthetic Aperture Radar Signal Processing*. Wiley, 1999.
- [16] A. Khwaja, L. Ferro-Famil, and E. Pottier, "SAR raw data simulation using high precision focusing methods," *European Radar Conference*, pp. 33–36, 2005.